Cellular/Molecular

Intracellular Domains of NMDA Receptor Subtypes Are Determinants for Long-Term Potentiation Induction

Georg Köhr,[1] Vidar Jensen,[3] Helmut J. Koester,[2] Andre L. A. Mihaljevic,[1] Jo K. Utvik,[4] Ane Kvello,[3] Ole P. Ottersen,[4] Peter H. Seeburg,[1] Rolf Sprengel,[1] and Øivind Hvalby[3]

[1]Max-Planck-Institute for Medical Research, D-69120 Heidelberg, Germany, [2]Baylor College of Medicine, Houston, Texas 77030, and [3]Institute of Basic Medical Sciences and [4]Centre for Molecular Biology and Neuroscience and Department of Anatomy, University of Oslo, N-0317 Oslo, Norway

NMDA receptors (NMDARs) are essential for modulating synaptic strength at central synapses. At hippocampal CA3-to-CA1 synapses of adult mice, different NMDAR subtypes with distinct functionality assemble from NR1 with NR2A and/or NR2B subunits. Here we investigated the role of these NMDA receptor subtypes in long-term potentiation (LTP) induction. Because of the higher NR2B contribution in the young hippocampus, LTP of extracellular field potentials could be enhanced by repeated tetanic stimulation in young but not in adult mice. Similarly, NR2B-specific antagonists reduced LTP in young but only marginally in adult wild-type mice, further demonstrating that in mature CA3-to-CA1 connections LTP induction results primarily from NR2A-type signaling. This finding is also supported by gene-targeted mutant mice expressing C-terminally truncated NR2A subunits, which participate in synaptic NMDAR channel formation and Ca^{2+} signaling, as indicated by immunopurified synaptic receptors, postembedding immunogold labeling, and spinous Ca^{2+} transients in the presence of NR2B blockers. These blockers abolished LTP in the mutant at all ages, revealing that, without the intracellular C-terminal domain, NR2A-type receptors are deficient in LTP signaling. Without NR2B blockade, CA3-to-CA1 LTP was more strongly reduced in adult than young mutant mice but could be restored to wild-type levels by repeated tetanic stimulation. Thus, besides NMDA receptor-mediated Ca^{2+} influx, subtype-specific signaling is critical for LTP induction, with the intracellular C-terminal domain of the NR2 subunits directing signaling pathways with an age-dependent preference.

Key words: **gene-targeted mouse; hippocampal CA3-to-CA1 LTP; postembedding immunogold labeling; coimmunoprecipitation; NR2B antagonists; two-photon imaging; spinous calcium transients; signal transduction**

Introduction

Functional NMDA receptor (NMDAR) complexes consist of many different proteins, including the receptor subunits (NR1 and NR2A–NR2D), adaptor proteins, signaling proteins, cytoskeletal proteins, and cell adhesion proteins (Husi et al., 2000; Walikonis et al., 2000). Protein–protein interactions within these complexes subserve trafficking, subcellular localization, clustering, and signal transduction of NMDARs (Kennedy, 2000; Sheng and Pak, 2000). The NMDAR ion channel mediates currents with NR2 subunit-dependent kinetics (Dingledine et al., 1999). During development, the NMDAR subunit composition changes in many brain regions and contributes to experience-dependent plasticity. The developmentally regulated increase in the NR2A subunit accelerates postsynaptic NMDAR current kinetics (Carmignoto and Vicini, 1992; Flint et al., 1997), but the presence of particular NR2 subunits appears to be more important than changes of current kinetics for plasticity during the critical period in the barrel cortex (Barth and Malenka, 2001; H. C. Lu et al., 2001) and visual cortex (Philpot et al., 2001; Fagiolini et al., 2003; Yoshimura et al., 2003).

Recent *in vitro* results suggest differential NMDAR signaling based on subcellular receptor localization. Extrasynaptic compared with synaptic NMDARs have a higher rate of use-dependent turnover attributable to differential regulation by intracellular proteins in microisland cultures (Li et al., 2002), and activation of synaptic versus extrasynaptic NMDARs differentially drives endocytosis of AMPARs in hippocampal cells (W. Lu et al., 2001). Furthermore, in hippocampal cultures, extrasynaptic but not synaptic NMDARs were found to be coupled to CREB (cAMP response element binding) shut-off and cell death pathways (Hardingham et al., 2002). However, in cortical cultures, synaptically and extrasynaptically activated NMDARs were reported to be equally capable of mediating excitotoxicity (Sattler et al., 2000).

Biochemical and anatomical data indicate that NMDARs are enriched in postsynaptic densities (PSDs) of hippocampal and cortical synapses (He et al., 1998; Petralia et al., 1999; Takumi et al., 1999; Nusser, 2000; Racca et al., 2000; Valtschanoff and Weinberg, 2001). NR2 subunits together with NR1 form the different NR2A- and NR2B-type NMDARs that contribute to synaptic responses in the hippocampus (Kirson and Yaari, 1996). Here we

Received Aug. 20, 2003; revised Sept. 12, 2003; accepted Sept. 22, 2003.

This work was supported in part by Deutsche Forschungsgemeinschaft Grant Ko 1064, the Norwegian Research Council, European Cooperation in Scientific and Technological Research, and European Union Biomed projects QLG3-CT-2001-02089 and QLRT-1999-01022. We thank Prof. P. Andersen and Dr. P. Osten for critically reading this manuscript, Prof. F. M. S. Haug for help with EM quantifications, and Prof. P. Laake with statistics.

Correspondence should be addressed to Dr. Georg Köhr, Department of Molecular Neurobiology, Max-Planck-Institute for Medical Research, Jahnstrasse 29, D-69120 Heidelberg, Germany. E-mail: kohr@mpimf-heidelberg.mpg.de.

 0270-6474/03/2310791-09$15.00/0

analyzed whether synaptically localized NMDARs mediate subtype-specific signaling. We used the functional requirement of NMDARs for long-term potentiation (LTP) induction at CA3-to-CA1 synapses (Bliss and Collingridge, 1993; Malenka and Nicoll, 1999) to evaluate differential signaling of NR2A- and NR2B-type receptors. By using NR2B-specific antagonists and a genetically altered mouse line in which the intracellular C-terminal domain of the endogenous NR2A subunit was truncated (Sprengel et al., 1998; Steigerwald et al., 2000), we show that the NR2A- and NR2B-type NMDARs contribute differently to LTP induction at CA3-to-CA1 synapses. Because the deletion of the intracellular C-terminal domain failed to activate the NR2A-specific pathway, despite channel formation, synaptic localization, and Ca^{2+} signaling of NR2AΔC-containing NMDARs, we postulate that the intracellular C-terminal domain of the NR2 subunits is a key determinant for downstream signaling.

Materials and Methods

Electrophysiology. Mice were killed with halothane. Transverse slices (400 μm) were cut with a vibroslicer from the middle portion of each hippocampus in the following artificial CSF (ACSF) (4°C, bubbled with 95% O_2–5% CO_2, pH 7.4; in mM): 124 NaCl, 2 KCl, 1.25 KH_2PO_4, 2 $MgSO_4$, 1 $CaCl_2$, 26 $NaHCO_3$, and 12 glucose. Slices were placed in a humidified interface chamber at 28–32°C and perfused with ACSF containing 2 mM $CaCl_2$. Some experiments used (−)-bicuculline methochloride (10 μM; Tocris Cookson, Bristol, UK) to facilitate LTP induction. Hyperexcitability was counteracted by increasing Ca^{2+} and Mg^{2+} to 4 mM. The NR2B subunit-specific antagonists were CP-101,606 (CP) (gift from Pfizer, Groton, CT) and Conantokin G (Con G) (Bachem, Bubendorf, Switzerland).

Orthodromic synaptic stimuli (50 μsec, <160 μA, 0.1 Hz) were delivered alternately through two tungsten electrodes placed in stratum radiatum and stratum oriens of CA1. Extracellular synaptic responses were monitored by glass electrodes (filled with ACSF) placed in the corresponding synaptic layers. After obtaining stable synaptic responses for at least 15 min in both pathways, one pathway was tetanized (with either a single 100 Hz tetanization for 1 sec or four such tetanizations given at 5 min intervals). The stimulation strength used for tetanization was set just above threshold for generation of a population spike in response to a single test shock. The synaptic efficacy was assessed by measuring the slope of the field EPSP in the middle third of its rising phase. Six consecutive responses (1 min) were averaged and normalized to the mean value recorded 1–4 min before tetanization. Data were pooled across animals of the same age and genotype and are presented as mean ± SEM. Statistical significance was evaluated by two-tailed *t* test.

Subcellular fractionation and coimmunoprecipitation. Subcellular fractionation (Gurd and Mahler, 1974) was performed using the protocol of Blahos and Wenthold (1996) from forebrains of 12 wild-type (WT) and 12 $NR2A^{\Delta C/\Delta C}$ mice [postnatal day 42 (P42)] in four independent preparations (three forebrains each). The resulting fractions were homogenates, cytosolic and microsomal fractions, and synaptosomes. Synaptosomes were resuspended in 50 mM Tris-HCl, pH 9.0, protease inhibitors (Complete; Roche Products), and deoxycholate was added to a final concentration of 1%, pH 9.0, for 1 hr at 37°C to solubilize 30–40% of the NMDARs as described previously (Blahos and Wenthold, 1996). The supernatant (100,000 × *g* at 4°C for 1 hr) was adjusted to 0.1% Triton X-100 and dialyzed overnight against 50 mM Tris-HCl, pH 7.5, 0.1% Triton X-100, and 0.32 M sucrose at 4°C using the dialyzing membrane MWC 12–14 kDa from Biomol (Hamburg, Germany). The dialyzed fraction was again centrifuged at 100,000 × *g* at 4°C for 1 hr.

The amount of NMDAR protein in synaptosome fractions was analyzed between wild-type and $NR2A^{\Delta C/\Delta C}$ mice by Western blot analysis on 8% polyacrylamide gels (Laemmli, 1970). Primary antibodies and dilutions were as follows: α-NR1 C terminal (mouse; PharMingen, San Diego, CA), 1:1000; α-NR2B C terminal (mouse; Novus Biologicals, Littleton, CO), 1:1000; α-NR2A N terminal [mouse, 2H9 (Boehringer Mannheim, Mannheim, Germany); ascites production (Eurogentec, Seraing, Belgium)], 1:500; α-PSD-95 (mouse; Upstate Biotechnology, Lake Placid, NY), 1:000; α-calnexin (rat; Stressgen); and α-β-actin (mouse; Sigma, St. Louis, MO), 1:20000. Secondary antibodies were either peroxidase-labeled α-mouse or α-rabbit at 1:15000 (Jackson ImmunoResearch, West Grove, PA). Signals were generated using ECLplus (Amersham Biosciences, Arlington Heights, IL).

For coimmunoprecipitation, we used α-NR1 C terminal (rabbit; Upstate Biotechnology), α-NR2B C terminal (rabbit; Chemicon, Temecula, CA), and α-NR2A N terminal (mouse, 2H9; see above), which precipitated in synaptosome fractions 30–50% of the NR1, NR2B, and NR2A complexes, respectively. Immunoprecipitated proteins were analyzed by Western blot analysis of 10% gels (primary and secondary antibodies and dilutions; see above). After ECLplus detection (Amersham Biosciences), each blot was exposed 8–10 times with different exposure times (ranging from seconds to minutes to ensure linearity). For each blot, different exposure times were scanned with Twain Pro (EPSON), 24 bit color scan and 800 dots per inch, and analysis was with Image Gauge (version 3.0; Fuji, Aichi, Japan). In α-NR1 immunoprecipitations (IPs), the signal intensities (*I*) of NRA and NR2B were corrected for background before calculating the ratio of NR2A versus NR2B: $I(\alpha\text{-NR2A}_{\Delta C/\Delta C})/I(\alpha\text{-NR2B}_{\Delta C/\Delta C})$ compared with $I(\alpha\text{-NR2A}_{WT})/I(\alpha\text{-NR2B}_{WT})$ analyzed in the same NR2A and NRB immunoblot, respectively. In α-NR2B IPs, the signal intensities (*I*) of NR1 and NR2A were corrected for background before calculating the ratio of NR1 versus NR2A in accordance with the above formula. Data are presented as mean ± SD.

Postembedding immunocytochemistry. All experiments were performed in accordance with the Norwegian Committee on Animal Experimentation. Four wild-type and four $NR2A^{\Delta C/\Delta C}$ mice (P35) were deeply anesthetized and transcardially perfused (Nagelhus et al., 1998; Rossi et al., 2002). Specimens containing the CA1 region were subjected to freeze substitution and were embedded in Lowicryl HM 20 (Matsubara et al., 1996). Ultrathin sections (~70 nm) were mounted on nickel grids and immunolabeled as described previously (Matsubara et al., 1996; Nagelhus et al., 1998; Takumi et al., 1999; Rossi et al., 2002) with antibodies against PSD-95 (rabbit; gift from Masahiko Watanabe, Hokkaido University, Hokkaido, Japan), the C-terminal end of NR1 (rabbit; gift from Robert Wenthold, National Institutes of Health, Bethesda, MD), the N-terminal end of NR2A (mouse, 2H9; see above), or the C-terminal end of NR2B (rabbit; Chemicon). The final concentrations were as follows: 2 μg/ml for NR1 and PSD-95; 10 μg/ml for NR2A and NR2B. All antisera have been characterized previously (NR1, Petralia et al., 1999; NR2A, Laurie et al., 1997; NR2B, Khan et al., 1999; PSD-95, Fukaya and Watanabe, 2000), and the specificity of the NR2A and NR2B antibodies was verified in transfected cell lines (data not shown). On the next day, the sections were incubated for 1–2 hr with goat anti-rabbit or goat anti-mouse Fab fragments coupled to 10 nm gold particles (GFAR10 and GFAM10, respectively; British BioCell International, Cardiff, UK) diluted 1:20. All incubations were in 5 mM Tris buffer containing 50 mM glycine, 0.3% NaCl, 0.01% (NR2B) or 0.1% Triton X-100, 2% human serum albumin, and (in the case of NR2A) 0.25% fish skin gelatin.

For all antibodies, quantified sections from all eight animals were investigated. Comparisons were made between sections incubated in the same drops of immunoreagents and did not involve serially reconstructed synapses. To determine the percentage of labeled PSD profiles and perisynaptic membranes in the basal part of stratum radiatum of CA1, the grid squares were systematically analyzed in the electron microscope (Rossi et al., 2002). A gold particle was considered associated with a specific profile if located within ±20 nm of the postsynaptic or perisynaptic membrane (the latter defined as the 200-nm-wide membrane domain starting 20 nm from the end and encircling the PSD). PSD lengths are presented as mean ± SD, and the proportion of immunolabeled profiles is given as percentage of the total number of profiles. Analysis of contingency tables and Pearson's χ^2 test were used to reveal the differences between the groups. The mean linear density is given as gold particles per micrometer of profile, and differences were tested by Mann–Whitney test.

Only a minor fraction of the NMDAR pool in a given synapse will be exposed at the surface of a section and is available for immunolabeling. The proportion of labeled profiles will thus be much smaller than the

proportion of asymmetric synapses expressing NMDARs (which is close to 100%) (Takumi et al., 1999), and the failure to detect NR1, NR2A, or NR2B in a single synaptic profile must not be taken as indication for their absence from the synapse but for a number of NMDAR below the detection limit for the immunogold procedure. However, because the likelihood of detecting a receptor in a single ultrathin section will increase with increasing receptor concentration, the proportion of labeled profiles will be a measure of the total receptor pool in the synapse.

Two-photon imaging. Four wild-type and six NR2A$^{\Delta C/\Delta C}$ mice (P42) were anesthetized by injection of ketamine, xylazine, and acepromazine, and transerve slices (250 μm) of the hippocampus were cut using a vibroslicer. All experimental procedures were approved by the Animal Research Committee of Baylor College of Medicine. The bathing solution contained 125 mM NaCl, 2.5 mM KCl, 1.25 mM NaH_2PO_4, 25 mM $NaHCO_3$, 2 mM $CaCl_2$, 1 mM $MgCl_2$, and 10 mM dextrose bubbled with 95% O_2–5% CO_2 at 34–36°C. CA1 cells were filled with Oregon Green 488 BAPTA-1 (OGB-1) (200 μM). EPSPs were evoked by placing a stimulation electrode in close proximity (5–10 μm) of a secondary oblique dendrite 50–350 μm from the soma. The stimulation strength was set to evoke a subthreshold EPSP of 1–8 mV. Spinous Ca^{2+} transients were recorded with multiphoton microscopy as described previously (Koester and Sakmann, 1998), and amplitudes are given by the maximal fluorescence increase relative to basal fluorescence ($\Delta F/F$). CP perfusion had no effect on EPSP amplitudes (control, 6.7 ± 0 mV; CP, 7.3 ± 1.4 mV; n = 6), precluding a change in synaptic transmission (e.g., presynaptically). Data are presented as mean ± SD, and differences were tested by a t test.

Results

NR2A-type NMDARs induce hippocampal LTP in adult mice

The NR2A- and NR2B-type NMDAR contribution in LTP induction at CA3-to-CA1 synapses was addressed by recordings in hippocampal slices from young (P14) and adult (>P42) mice in the presence or absence of NR2B subunit-specific antagonists. CP is a noncompetitive antagonist that binds with high affinity to heterodimeric NR1/NR2B receptors but not to NR1/NR2A or heterotrimeric NR1/NR2A/NR2B receptors and efficiently blocks NMDARs in developing neurons (Stocca and Vicini, 1998; Chazot et al., 2002). Con G is a competitive antagonist that does not block NR1/NR2A but NR1/NR2B and, partially, heterotrimeric NR1/NR2A/NR2B (Donevan and McCabe, 2000; Klein et al., 2001).

In slices of P14 mice, 40–45 min after a single tetanization of the afferent fibers in either stratum radiatum or stratum oriens, we observed robust LTP of extracellular field potentials that was NMDAR dependent (data not illustrated). The average slope of the field EPSP was 1.32 ± 0.05 (mean ± SEM; n = 29), whereas the synaptic transmission in the untetanized control pathway was unchanged (Fig. 1*A*). LTP elicited by four tetanic stimulations, given at 5 min intervals, was significantly larger (1.58 ± 0.09; n = 13; p = 0.01) (Fig. 1*A*). This difference in LTP was abolished by 10 μM CP, demonstrating that, at this age, NR1/NR2B receptors contribute to LTP induction in a stimulus-dependent manner (1.37 ± 0.09; n = 14) (Fig. 1*A*).

In slices of adult mice, in contrast to P14, single tetanization was as efficient as repeated tetanizations in inducing LTP (1.39 ± 0.07, n = 22 vs 1.51 ± 0.07, n = 17; p = 0.22) (Fig. 1*B*). Moreover, the magnitude of LTP was unaffected by CP, which indicates that, in adult mice, NR1/NR2B receptors have a minor, if any, contribution to LTP induction under the condition used (1 × 100 Hz, 1.39 ± 0.05, n = 19, p = 0.99; 4 × 100 Hz, 1.44 ± 0.08, n = 17, p = 0.44) (Fig. 1*B*). Con G (3 μM) reduced the magnitude of LTP after repeated tetanization at P42 to 1.28 ± 0.10 (n = 10; p = 0.04; data not shown), suggesting also that NR1/NR2A/NR2B receptors participated in LTP induction.

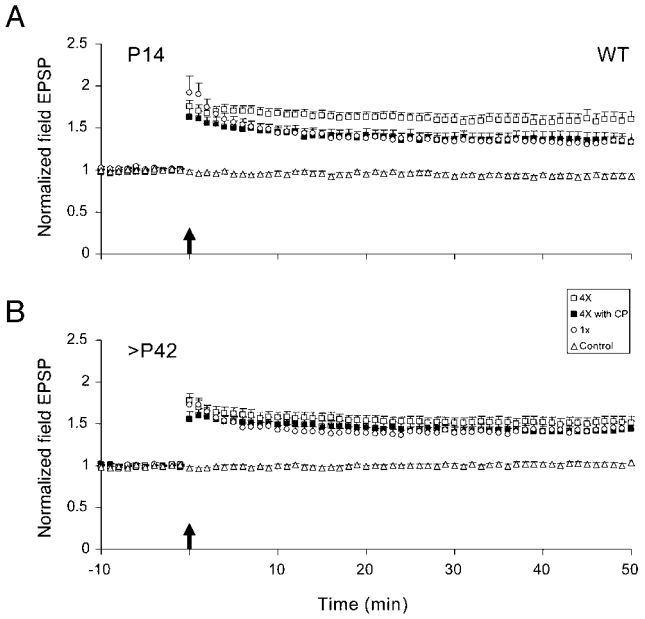

Figure 1. LTP in CA1 is mediated by NR2A- and NR2B-type NMDARs in juvenile (*A*; P14) and NR2A-type NMDARs in adult (*B*; >P42) wild-type mice. LTP of EPSPs was induced by a single tetanization (open circles) or by four tetanizations in the absence and presence of the NR2B subunit-specific antagonist CP-101,606 (open and filled squares, respectively). Open triangles show the untetanized control pathway from single tetanization experiments. For experiments using CP during a single tetanization and using the NR2B subunit-specific antagonist Con G, see Results. To compare the results of the two tetanization paradigms, the period between the first and the fourth tetanization (15 min) has been removed. The arrows indicate the time of both the first and the fourth tetanic stimulation. Data are the mean ± SEM.

Thus, in adult mice, the NR2A subunit is primarily responsible for LTP induction, independent of the tetanization paradigm.

In NMDAR complexes at postsynaptic sites, C-terminally truncated NR2A subunits assemble with NR1 and NR2B

The prevailing view that NR2A-containing NMDARs induce LTP in mature CA3-to-CA1 synapses is also supported by NR2A knock-out mice (Sakimura et al., 1995) and, as expected from our pharmacological results, show strongly reduced CA3-to-CA1 LTP. A similar reduction in LTP was observed in mice just lacking the C-terminal, cytoplasmatic domain of the NR2A protein (NR2A$^{\Delta C/\Delta C}$) (Sprengel et al., 1998). In contrast to NR2A knock-out mice that lack NR2A-type receptors, NR2A$^{\Delta C/\Delta C}$ mice express NR2A-type NMDARs that are still active but reduced in number at hippocampal synapses (Steigerwald et al., 2000). This suggested a functional importance of the NR2A C-terminal domain in LTP signaling at mature CA3-to-CA1 synapses.

To investigate NR2A-type NMDARs at synaptic sites by biochemical means, we analyzed NMDAR complexes in forebrain extracts. As in our previous work (Steigerwald et al., 2000), synaptosomes of NR2A$^{\Delta C/\Delta C}$ mice show regular enrichment of NR1, NR2B, and PSD-95 proteins, whereas the enrichment of the C-terminally truncated NR2A subunit is reduced when compared with NR2A in wild-type mice (Fig. 2*A*). Furthermore, NR1 and NR2B levels are comparable in synaptosomes of both genotypes, whereas the level of NR2AΔC is reduced (~40% of wild-type mice; also indicated by Steigerwald et al., 2000). The C-terminally truncated NR2A subunit remains assembled with NR1 and NR2B subunits, because C-terminal anti-NR1 as well as anti-NR2B antibodies coprecipitated the NR2A subunit in wild-type and NR2A$^{\Delta C/\Delta C}$ mice (Fig. 2*B*). NR1 complexes were pre-

cipitated from three different synaptosome preparations, and the NR2A/2B ratio within these complexes was reduced by ~70% in NR2A$^{\Delta C/\Delta C}$ mice (0.27 ± 0.02; $n = 3$) (for quantification, see Materials and Methods) when compared with NR2A/2B ratios in wild type (Fig. 2*B*). However, this reduction also reflects decreased stability of NR2AΔC-containing NMDAR complexes, because an N-terminal NR2A antibody coprecipitated less NR1 from synaptosomes of NR2A$^{\Delta C/\Delta C}$ compared with wild type (Fig. 2*B*). Therefore, the number of NR2A-containing NMDAR complexes in NR2A$^{\Delta C/\Delta C}$ mice is likely to exceed that indicated by immunoprecipitated NR1 complexes. The NR2A/NR1 ratio in immunoprecipitated NR2B complexes of NR2A$^{\Delta C/\Delta C}$ mice was only reduced by ~20% compared with wild type (0.80 ± 0.17; $n = 4$), suggesting that, in NR2A$^{\Delta C/\Delta C}$ mice, heterotrimeric NMDARs may be more stable than heterodimeric NMDARs. Importantly, our analysis of synaptosomes indicates that the C-terminal truncated NR2A subunits remain assembled in NMDAR complexes.

Our biochemical data provided additional proof that C-terminally truncated NR2A subunits are incorporated in synaptically localized NMDARs. However, the difference in receptor stability perturbed efforts of exact quantification of NMDARs in the synapse. Therefore, we performed exact morphological localization of NMDARs by quantitative immunogold analysis in PSDs.

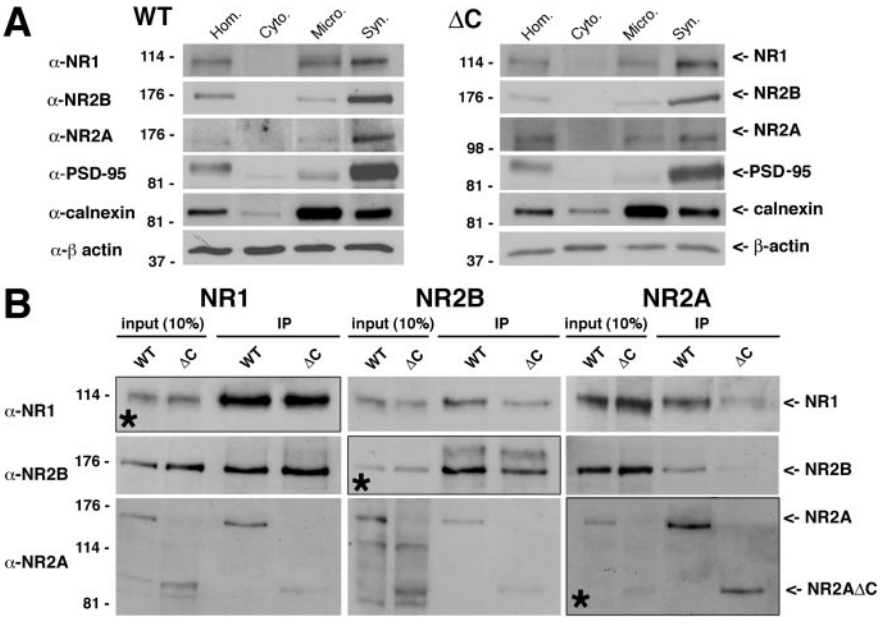

Figure 2. In NMDAR complexes of synaptosomes, C-terminally truncated NR2A subunits assemble with NR1 and NR2B. *A*, Subcellular fractions of synaptosome preparations (Hom., homogenates; Cyto., cytosolic; Micro., microsomal; Syn., synaptosomal) from forebrains of wild-type (left) and NR2A$^{\Delta C/\Delta C}$ (right) mice were analyzed in immunoblots for the presence of NR1, NR2B, NR2A, PSD-95, calnexin, and β-actin. β-Actin was used to control that equal amounts of protein (10 μg) were loaded on the gel. PSD-95, NR1, NR2B, and NR2A are enriched in synaptosomes, and calnexin is enriched in microsomes. Synaptosomes of NR2A$^{\Delta C/\Delta C}$ mice showed impaired enrichment for NR2AΔC compared with NR2A of wild-type mice. *B*, NMDAR complexes of synaptosome fractions were immunoprecipitated (IP) with antibodies recognizing the C terminus of NR1 and NR2B or the N terminus of the NR2A subunit. Ten percent of the input and immunoprecipitated samples were analyzed in immunoblots for the presence of NR1, NR2B, and NR2A subunits. Immunoblots that were performed with the same antibody used in the IPs are boxed and marked by a star. These IPs show a threefold to fivefold stronger signal intensity than the 10% input, indicating an IP efficacy of 30–50% depending on the amount of antibody used in the reaction. Immunoblots for the coassembled subunits of immunoprecipitated NMDAR complexes show that 5–10% of the precipitated subunit remain associated with coassembled subunit during the immunoprecipitation (for NR2A IPs of NR2A$^{\Delta C/\Delta C}$ mice; see Results). In synaptosomes of both wild-type and NR2A$^{\Delta C/\Delta C}$ mice, the anti-NR1 IP copurified the subunits NR2A and NR2B, the anti-NR2B IP copurified subunits NR1 and NR2A, and the anti-NR2A IP copurified subunits NR1 and NR2B. The normalized ratio of the copurified NMDAR subunits was used to evaluate their relative levels within NMDAR complexes of wild-type and NR2A$^{\Delta C/\Delta C}$ mice.

Synaptic structures and PSDs were comparable in wild-type and NR2A$^{\Delta C/\Delta C}$ mice, because PSD profiles showed similar average lengths (206.0 ± 58.2 nm, $n = 790$; 206.4 ± 62.6 nm, $n = 1018$; $p = 0.9$) as well as similar PSD-95 (Fig. 3*A*) and NR1 and NR2B immunosignals (Fig. 3*C*). The percentage of PSD profiles with one or more α-NR1 immunogold particles was 75.2 and 70.5% ($p = 0.27$), and the mean linear densities of NR1 immunogold particles for positive labeled profiles were 8.79 and 7.26 gold particles/μm ($p = 0.09$) in wild-type and NR2A$^{\Delta C/\Delta C}$ mice, respectively. The NR2B-specific immunogold signal provided a similar result, and 62.9 and 62.4% ($p = 0.90$) of the PSD profiles were labeled with ~8.02 and 7.27 gold particles/μm ($p = 0.77$) in wild-type and NR2A$^{\Delta C/\Delta C}$ mice, respectively. Also in the perisynaptic profiles, the NR1 and NR2B immunogold values did not reflect a difference in the NMDAR distribution between both genotypes with 10.2 and 11.2% NR1 ($p = 0.65$) and 7.8 and 7.3% NR2B ($p = 0.77$) immunogold-labeled profiles, indicating that most perisynaptic profiles were unlabeled in wild-type and NR2A$^{\Delta C/\Delta C}$ mice. The mean linear particle density was 5.19 and 5.05 gold particles/μm ($p = 0.42$) for NR1 and 4.72 and 4.78 gold particles/μm ($p = 0.18$) for NR2B in wild-type and NR2A$^{\Delta C/\Delta C}$ mice, respectively.

However, a difference in the NMDAR distribution was detected in NR2A$^{\Delta C/\Delta C}$ mice when an NR2A-specific antibody was used that interacts with the N-terminal domain of the NR2A subunit and that identifies the 180 kDa NR2A subunit as single band in immunoblots of PSDs from forebrains of wild-type mice (Steigerwald et al., 2000). In wild type, 52.3% of the PSD profiles were labeled by anti-NR2A immunogold, whereas only 28% were labeled in NR2A$^{\Delta C/\Delta C}$ mice (Fig. 3*B*,*C*). This reduction in NR2A-labeled PSD profiles by ~45% ($p < 0.0005$) is consistent with the reduced level of NR2A protein observed in synaptosomes of forebrains (see above). Thus, the reduced level of NR2A protein in NR2A$^{\Delta C/\Delta C}$ mice seems to affect the number of NR2A-containing synapses without affecting the number of NR2A-containing receptors per synapse. This result is supported in NR2A immunopositive profiles by the mean linear immunogold particle density, which was not different between wild-type and NR2A$^{\Delta C/\Delta C}$ mice (6.12 and 5.67 particles/μm; $p = 0.28$), confirming a similar number of NR2A-containing receptors in anti-NR2A-labeled synapses of both genotypes. As for NR1 and NR2B, most perisynaptic profiles were unlabeled for NR2A (Fig. 3*C*). In wild-type and NR2A$^{\Delta C/\Delta C}$ mice, 8.4 and 9.9% ($p = 0.267$) of the perisynaptic profiles were labeled. The linear density of gold particles in positive perisynaptic profiles of NR2A$^{\Delta C/\Delta C}$ mice was significantly increased to 4.18 gold particles/μm (WT, 3.71 gold particles/μm; $p = 0.004$), reflecting the reduced synaptic enrichment of NR2AΔC (see above). Thus, NR2A$^{\Delta C/\Delta C}$ mice contain fewer NR2A-positive synapses, but the positive synapses exhibit regular number and subsynaptic distribution of NR2A-containing receptors.

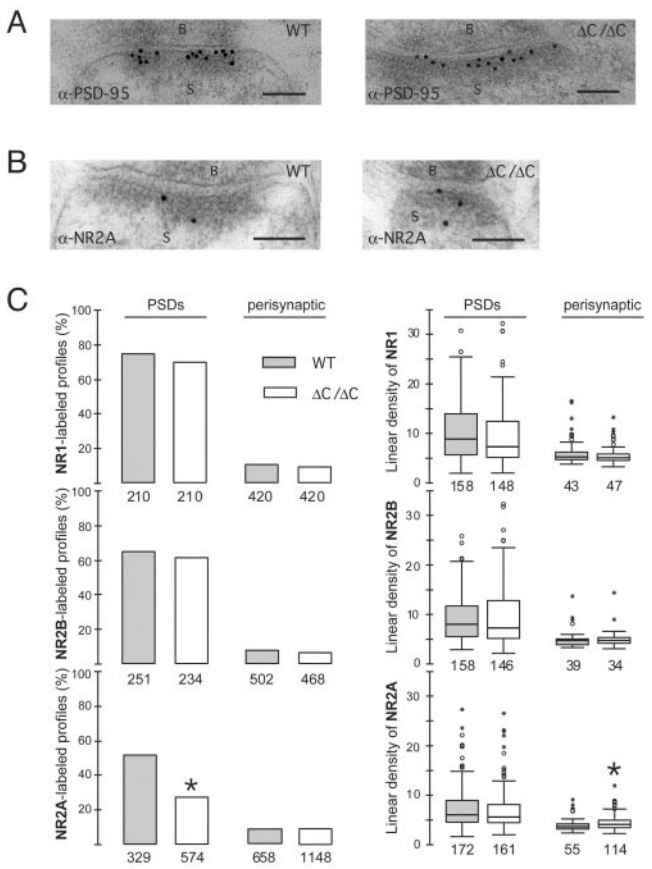

Figure 3. NR2AΔC is present in postsynaptic densities of NR2A$^{\Delta C/\Delta C}$ mice. Immunogold labeling of PSD-95 (*A*) or NR2A (*B*) in stratum radiatum of CA1 of wild-type (WT) and NR2A$^{\Delta C/\Delta C}$ mice (ΔC/ΔC). In each panel, B and S mark bouton and spine. Scale bar, 100 nm. *C*, Quantitation of NR1, NR2B, and NR2A labeling in PSDs and perisynaptic regions. NR1 and NR2B were similarly distributed in both genotypes. Truncation of NR2A caused a reduction (*$p < 0.0005$; analysis of contingency tables and Pearson's χ^2 test) in the proportion of NR2A-labeled PSD profiles (i.e., profiles associated with ≥1 gold particle; mean ± SD). However, profiles that remained labeled showed the same median linear gold particle density (linear density is particles per micrometer of membrane) as the population of profiles that were labeled in wild type. There was no change in the proportion of labeled perisynaptic profiles, although the latter profiles showed a small increase (*$p = 0.004$; Mann–Whitney test) in the linear median gold particle density in NR2A$^{\Delta C/\Delta C}$ mice. The linear density plot is based on the median, quartiles, and extreme values. Boxes represent the interquartile range that contains 50% of values. The whiskers represent maximum and minimum values, excluding outliers (circles, between 1.5 and 3 box lengths from top or bottom edge of box) and extremes (asterisks, >3 box lengths from the edge of the box). The line across the box indicates the median. Numbers of profiles are indicated.

In summary, CA1 synapses in NR2A$^{\Delta C/\Delta C}$ mice appear normal. They show normal levels of PSD-95, NR1, and NR2B, but the number of NR2A-containing synapses is reduced. Thus, despite the lack of the C-terminal NR2A domain, at least half of the CA1 synapses in NR2A$^{\Delta C/\Delta C}$ mice contain NR2A.

Spinous Ca^{2+} signals in CA1 pyramidal cells of NR2A$^{\Delta C/\Delta C}$ and wild-type mice (P42)

NR2A-type NMDARs of NR2A$^{\Delta C/\Delta C}$ mice participate during synaptic transmission in CA3-to-CA1 synapses, as demonstrated by electrophysiological recordings (Steigerwald et al., 2000). Now we analyzed spinous Ca^{2+} responses by multiphoton laser scanning microscopy (Koester and Sakmann, 1998) to evaluate the Ca^{2+} signaling of C-terminally truncated NR2A-type receptors in CA1 cells. To dissect Ca^{2+} influx through NMDARs from other sources (e.g., voltage-dependent calcium channels) we elicited single subthreshold EPSPs via an extracellular stimulating electrode and recorded Ca^{2+} transients in dendritic spines (Fig. 4*A*,*B*). Under these conditions, Ca^{2+} signals are blocked by the NMDAR antagonist AP-5 (50 μM) (Zamanillo et al., 1999). We did not examine Ca^{2+} transients evoked by trains of stimuli, which easily saturate the high-affinity indicator OGB-1. When using the low-affinity indicator OGB-5N, we were not able to find activated spine(s), because the Ca^{2+} fluorescence transient evoked by a single stimulus was barely distinguishable from the noise of the recordings.

As expected from the unchanged number of NR2A-type receptors per NR2A-positive synapse in NR2A$^{\Delta C/\Delta C}$ mice (see above), Ca^{2+} transients were as large as in wild type, at least in some spines of NR2A$^{\Delta C/\Delta C}$ mice (Fig. 4*C*). Other spines of NR2A$^{\Delta C/\Delta C}$ mice showed very small Ca^{2+} transients that were not detected in wild type, in agreement with the increased number of synapses lacking NR2A in NR2A$^{\Delta C/\Delta C}$ mice. On average, spinous Ca^{2+} transients were reduced in NR2A$^{\Delta C/\Delta C}$ mice by ~30% compared with wild-type mice ($\Delta F/F$; WT, 0.75 ± 0.23, $n = 32$; NR2A$^{\Delta C/\Delta C}$, 0.55 ± 0.22, $n = 55$; $p = 0.0002$). In this study, only the overall 30% reduction is relevant, because LTP was not investigated at single synapses.

NR2B blockade reduced spinous Ca^{2+} responses in both genotypes, indicating a contribution of NR2B-type NMDARs to Ca^{2+} signaling in both genotypes [$\Delta F/F$; WT plus CP, 0.47 ± 0.13, $n = 25$; NR2A$^{\Delta C/\Delta C}$ plus CP ($p = 0.0036$), 0.36 ± 0.14, $n = 36$] (Fig. 4*C*). However, the reduced Ca^{2+} transients in dendritic spines of NR2A$^{\Delta C/\Delta C}$ mice in the absence of CP were still larger ($p = 0.045$) than the Ca^{2+} signals recorded in the presence of CP in wild type. As mentioned above, this NR2B block was not sufficient to reduce LTP in wild type. Thus, NR2A-type receptors with C-terminally truncated NR2A subunits provide significant Ca^{2+} transients in the spine.

Hippocampal LTP in NR2A$^{\Delta C/\Delta C}$ mice is induced by NR2B-type NMDARs

NR2A-type NMDARs in NR2A$^{\Delta C/\Delta C}$ mice mediate reduced Ca^{2+} influx in dendritic spines, which might explain why LTP in NR2A$^{\Delta C/\Delta C}$ mice is reduced but not blocked (Sprengel et al., 1998). To further elucidate the contribution of NR2A-type signaling to LTP induction in NR2A$^{\Delta C/\Delta C}$ mice, we analyzed LTP in the absence and presence of NR2B blockers.

At P14, LTP in NR2A$^{\Delta C/\Delta C}$ mice after a single tetanization was not significantly reduced compared with that of age-matched wild-type mice (1.21 ± 0.03, $n = 25$; vs 1.32 ± 0.05, $n = 29$; $p = 0.09$) (Fig. 5*A*). Similar to wild type, repeated tetanization gave substantially more LTP than single tetanization (1.47 ± 0.10; $n = 12$; $p = 0.003$) (Fig. 5*A*), with LTP reaching wild-type levels ($p = 0.41$). In contrast to wild type, however, CP completely blocked LTP in NR2A$^{\Delta C/\Delta C}$ mice, suggesting that, at P14, LTP induction depends entirely on NR2B-containing NMDARs, if NR2A is present in its truncated form (tetanized vs control pathway, 1.01 ± 0.03 vs 0.96 ± 0.03; $n = 6$; $p = 0.24$) (Fig. 5*A*).

In adult NR2A$^{\Delta C/\Delta C}$ mice, as observed previously (Sprengel et al., 1998), LTP after a single tetanization was significantly reduced compared with wild-type mice (1.16 ± 0.04, $n = 28$, vs 1.39 ± 0.07, $n = 22$; $p = 0.003$) (Fig. 5*B*). The reduced LTP level might reflect suboptimal induction. Therefore, we blocked the $GABA_A$ receptor-mediated inhibition, which facilitates the induction of LTP without affecting its magnitude (Wigstrom and Gustafsson, 1985). In the presence of bicuculline (10 μM), LTP evoked by a single tetanization was not significantly different from LTP obtained in control solution, in neither NR2A$^{\Delta C/\Delta C}$

(1.19 ± 0.04; $n = 20$; $p = 0.59$) nor wild-type (1.33 ± 0.04; $n = 37$; $p = 0.41$) mice, indicating efficient LTP induction in both genotypes.

Consistent with the results from NR2A knock-out mice (Kiyama et al., 1998), repeated tetanization in adult NR2A$^{\Delta C/\Delta C}$ mice gave substantially more LTP than a single tetanization (1.46 ± 0.06; $n = 11$; $p = 0.00008$) (Fig. 5*B*), but the amount of LTP was similar to that in wild type ($p = 0.56$). CP blocked both LTP induced by single tetanization (tetanized pathway, 1.03 ± 0.03 vs control pathway, 0.98 ± 0.03; $n = 17$; $p = 0.13$) and repeated tetanizations (1.01 ± 0.04 vs 0.97 ± 0.03; $n = 16$; $p = 0.38$) (Fig. 5*B*). In addition, Con G (3 μM) completely blocked LTP induced by repeated tetanizations in NR2A$^{\Delta C/\Delta C}$ mice (tetanized pathway, 1.05 ± 0.07 vs control pathway, 1.04 ± 0.05; $n = 9$; $p = 0.77$). Collectively, these results indicate that, in NR2A$^{\Delta C/\Delta C}$ mice, NR2B-type NMDARs are exclusively responsible for LTP induction.

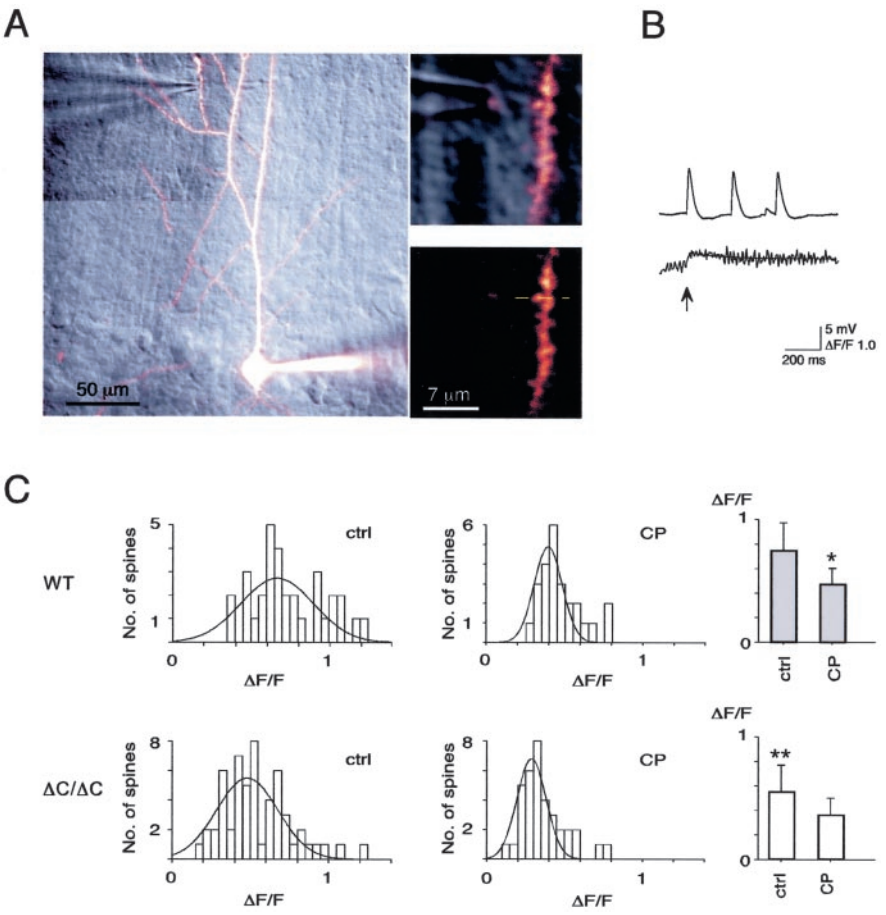

Figure 4. NR2A-type NMDARs in NR2A$^{\Delta C/\Delta C}$ mice mediate substantial spinous Ca^{2+} transients. *A*, Left, Overlay of a projection through a stack of two-photon images and a scanned Dodt-contrast image. Right top, Magnification of the left panel. Right bottom, Two-photon image of the examined dendrite; broken line indicates scan line. *B*, Extracellular, low-frequency stimulation evoked single EPSPs (top trace) and, in a stochastic manner, spinous Ca^{2+} signals (bottom trace, arrow). *C*, Histograms and averages (±SD) of Ca^{2+} signal amplitudes in wild-type (top) and NR2A$^{\Delta C/\Delta C}$ (bottom) mice in the absence (ctrl) and presence of CP ($p < 0.0001$; *t* test). Compared with wild-type (gray), spinous Ca^{2+} signals in NR2A$^{\Delta C/\Delta C}$ mice (white) were smaller in the absence of CP (**$p = 0.002$). These spinous Ca^{2+} signals in NR2A$^{\Delta C/\Delta C}$ mice were larger than Ca^{2+} signals in wild type in the presence of CP (*$p = 0.045$).

Discussion

The aim of the present study was to analyze the contribution of the NR2A- and NR2B-containing NMDARs to LTP induction at hippocampal CA3-to-CA1 synapses.

During early postnatal days, when signaling cascades for LTP induction switch (Yasuda et al., 2003) and NR2A expression is still not at peak (Monyer et al., 1994), hippocampal LTP is mediated via NR2B-containing NMDARs, consistent with the marginally reduced LTP in young NR2A knock-out (Ito et al., 1996) and NR2A$^{\Delta C/\Delta C}$ (this study) mice. At this developmental stage, LTP induced by single tetanization could be enhanced by four tetanizations. The latter increase was prevented by the NR2B blocker CP, indicating substantial contribution of NR2B-containing NMDARs to LTP induction during the maturation of the hippocampal circuitry. In adult mice, however, the NR2A-type NMDARs were found to be sufficient for the formation of LTP, because CP had no effect on the level of LTP induced by single or repeated tetanizations. Heterodimeric NR1/NRA and heterotrimeric NR1/NR2A/NR2B receptors could contribute to LTP induction as indicated by the partially reduced LTP in the presence of Con G. Thus, the NR2A-dependent pathway dominates in mediating tetanization-induced LTP at adult hippocampal synapses, although NR2B expression persists (Sans et al., 2000).

Here we show by immunogold that NR2A and NR2B are colocalized at the same CA1 synapses of 5-week-old wild-type mice. Approximately 52% of the synapses were NR2A positive, whereas 63% were NR2B positive in single sections. Thus, the percentage of colabeled synapses counting both NR2A and NR2B subunits is at least 15%. However, assuming that the number of labeled profiles is smaller than that of asymmetric synapses containing NMDARs (which is close to 100%) (Takumi et al., 1999), the number of colabeled synapses is expected to be higher. In NR2A$^{\Delta C/\Delta C}$ mice, NR2B was neither upregulated nor redistributed between synaptic and perisynaptic membranes. NR2AΔC remained constant in synapses of NR2A$^{\Delta C/\Delta C}$ mice but was present in fewer synaptic profiles than in wild type. This result is unlikely to reflect a general decrease in the NMDAR pool at all synapses, because the labeling density in the immunopositive synapses remained unchanged in both genotypes. Rather, the reduction in labeled PSD profiles in NR2A$^{\Delta C/\Delta C}$ mice could be explained by the reduced likelihood of detecting NR2A in a single section through the PSD because of the reduced amount of NR2A in NR2A$^{\Delta C/\Delta C}$ (see Materials and Methods). Our data are also consistent with two subpopulations of CA3-to-CA1 synapses (or a single population with a skewed distribution of receptor density) to which heterodimeric and heterotrimeric receptors may contribute at unknown relative abundance (Chazot et al., 1994; Sheng et al., 1994; Chazot and Stephenson, 1997; Luo et al., 1997; Tovar and Westbrook, 1999). Coimmunoprecipitation experiments using NR1, NR2B, or NR2A antibody indicate that NR2AΔC subunits remain assembled in NMDAR complexes. The reduced enrichment of NR2A-containing complexes at synaptic sites in NR2A$^{\Delta C/\Delta C}$ mice could be the result of lacking

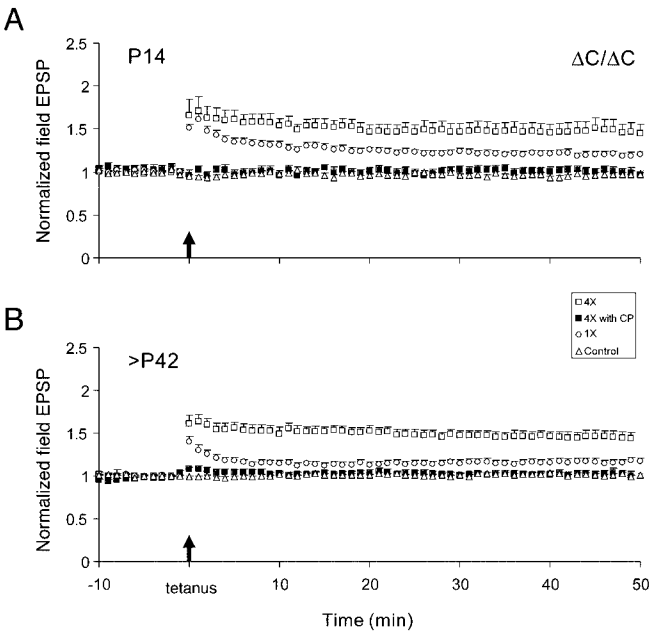

Figure 5. NR2B-type NMDARs mediate LTP in CA1 of juvenile (*A*; P14) and adult (*B*; >P42) NR2A$^{\Delta C/\Delta C}$ mice. LTP was induced by a single tetanization (open circles) or by four tetanizations in the absence and presence of the NR2B subunit-specific antagonist CP-101,606 (open and filled squares, respectively). Open triangles show the untetanized control pathway from single tetanization experiments. CP and Con G also completely blocked the development of LTP after a single tetanization and four tetanizations, respectively (see Results). The arrows indicate the time of both the first and the fourth tetanic stimulation.

C-terminal *t*SXV (since well known)-mediated (Kornau et al., 1995) PDZ (PSD-95/Discs-large/zona occludens-1) interactions (Kornau et al., 1995), as well as impaired delivery and/or anchoring mechanisms (Barria and Malinow, 2002; Sans et al., 2003).

The reduced synaptic presence of NR2AΔC-containing NMDARs in the mutant caused a modest reduction of spinous Ca^{2+} transients of ~30% relative to wild-type synapses, consistent with the 40% reduction of NR2AΔC in synaptosomes, the 45% reduction of NR2AΔC immunogold labeling in PSD profiles, and the 43% reduction of stimulus-evoked synaptic NMDA currents in NR2A$^{\Delta C/\Delta C}$ mice (Steigerwald et al., 2000, their Fig. 3*A*). This reduction of the postsynaptic Ca^{2+} transient might explain the lack of NR2A-type NMDAR-mediated LTP in NR2A$^{\Delta C/\Delta C}$ mice, given that NMDAR-mediated Ca^{2+} influx into spines and, in particular, its slow time course are major determinants of long-term effects on synaptic efficacy at hippocampal synapses (Yuste et al., 1999; Sabatini et al., 2002). However, the reduced spinous Ca^{2+} transient in adult NR2A$^{\Delta C/\Delta C}$ mice was comparable in magnitude with the spinous Ca^{2+} transient in wild type when the NR2B-type NMDAR was blocked. The same block did not affect LTP in adult wild-type mice. Thus, LTP was reduced in NR2A$^{\Delta C/\Delta C}$ mice, although NMDAR-mediated Ca^{2+} influx remained at levels sufficient to induce LTP in wild-type mice.

According to our results, both NR2A- and NR2B-type NMDARs activate signaling pathways, which lead to LTP. In young animals, both contribute to LTP, whereas in adult animals, NR2A-mediated signaling dominates. The reduced Ca^{2+} transients of stimulated CA1 neurons, when NR2B-type signaling is blocked, indicate that, in adult animals, NR2B-type NMDARs are still functional and, therefore, the NR2B-activated pathway appears to be operative in mature CA3-to-CA1 synapses. However, under the experimental condition used, the NR2A-type pathway is sufficient to induce LTP. When this pathway is eliminated by depletion of NR2A or removal of its C-terminal domain, the signaling by NR2B-type NMDARs is uncovered. It is likely that both NR2A- and NR2B-dependent LTP pathways are involved in memory formation in adult mice because, in contrast to mice that lack all NMDARs in CA1 pyramidal cells (McHugh et al., 1996), NR2A knock-out mice are less impaired in learning tests (Kiyama et al., 1998). The contribution of the NR2B-type pathway to learning and memory was demonstrated in mice overexpressing NR2B (Tang et al., 1999; Wong et al., 2002).

NR2A and NR2B may interact with different or the same signaling molecules. Preferential LTP induction by NR2A can occur in either scenario as the following examples indicate. Cdk5 (cyclin-dependent kinase-5) phosphorylates NR2A but not NR2B and appears to contribute to LTP in CA1 neurons by upregulating NMDAR activity (Li et al., 2001). Of the Src-family protein tyrosine kinases (Ali and Salter, 2001), fyn interacts with NR2A (Tezuka et al., 1999) and NR2B (Yaka et al., 2002), but tyrosine phosphorylation of NR2B could be controlled by the inhibitory scaffolding protein RACK1 (receptor for activated C kinase 1). RACK1 was detected in a trimolecular complex with fyn and NR2B but not NR2A and prevented tyrosine phosphorylation of NR2B, resulting in decreased NMDAR activity (Yaka et al., 2002). Therefore, in one scenario, repeated tetanization could be necessary to release RACK1 from NR2B or to uncouple any other negative effector pathway, e.g., PSD-95 (PSD-95 knock-out mice show enhanced LTP) (Migaud et al., 1998). It is also possible that preferential LTP induction by NR2A depends on interactions with neighboring receptors, adapter proteins with scaffolding functions, and/or cytoskeletal elements (Sheng and Kim, 2002), which are disrupted when the C-terminal domain is missing. On the other hand, spatiotemporal dynamics of NMDAR-mediated Ca^{2+} elevations may be perturbed in the absence of NR2A C-terminal interactions with intracellular proteins in NR2A$^{\Delta C/\Delta C}$ mice, and therefore Ca^{2+} signaling might fail during LTP induction.

To summarize, pharmacological experiments performed in developing wild-type mice indicate NMDAR subunit-specific, age-dependent signaling during LTP induction. Although synaptic NR2A expression was reduced in NR2A$^{\Delta C/\Delta C}$ mice, the effect on LTP could not be attributed to any gross changes in the organization of the synapse, as judged by ultrastructural characteristics and immunogold analyses of several synaptic proteins, including the NMDAR subunits and the NMDAR anchoring protein PSD-95. There was a reduced but sufficient Ca^{2+} influx in the postsynaptic elements of NR2A$^{\Delta C/\Delta C}$ mice. Thus, we propose that LTP induction is not only determined by NMDAR-mediated Ca^{2+} influx but by NR2-specific signaling mechanisms that depend on the integrity of the C terminus. These data find support in mice with brain-specific c-*fos* deletion, which show selective impairment of the NR2A pathway (Fleischmann et al., 2003).

References

Ali DW, Salter MW (2001) NMDA receptor regulation by Src kinase signalling in excitatory synaptic transmission and plasticity. Curr Opin Neurobiol 11:336–342.

Barria A, Malinow R (2002) Subunit-specific NMDA receptor trafficking to synapses. Neuron 35:345–353.

Barth AL, Malenka RC (2001) NMDAR EPSC kinetics do not regulate the critical period for LTP at thalamocortical synapses. Nat Neurosci 4:235–236.

Blahos II J, Wenthold RJ (1996) Relationship between *N*-methyl-D-

aspartate receptor NR1 splice variants and NR2 subunits. J Biol Chem 271:15669–15674.
Bliss TV, Collingridge GL (1993) A synaptic model of memory: long-term potentiation in the hippocampus. Nature 361:31–39.
Carmignoto G, Vicini S (1992) Activity-dependent decrease in NMDA receptor responses during development of the visual cortex. Science 258:1007–1011.
Chazot PL, Stephenson FA (1997) Biochemical evidence for the existence of a pool of unassembled C2 exon-containing NR1 subunits of the mammalian forebrain NMDA receptor. J Neurochem 68:507–516.
Chazot PL, Coleman SK, Cik M, Stephenson FA (1994) Molecular characterization of *N*-methyl-D-aspartate receptors expressed in mammalian cells yields evidence for the coexistence of three subunit types within a discrete receptor molecule. J Biol Chem 269:24403–24409.
Chazot PL, Lawrence S, Thompson CL (2002) Studies on the subtype selectivity of CP-101, 606: evidence for two classes of NR2B-selective NMDA receptor antagonists. Neuropharmacology 42:319–324.
Dingledine R, Borges K, Bowie D, Traynelis SF (1999) The glutamate receptor ion channels. Pharmacol Rev 51:7–61.
Donevan SD, McCabe RT (2000) Conantokin G is an NR2B-selective competitive antagonist of *N*-methyl-D-aspartate receptors. Mol Pharmacol 58:614–623.
Fagiolini M, Katagiri H, Miyamoto H, Mori H, Grant SG, Mishina M, Hensch TK (2003) Separable features of visual cortical plasticity revealed by *N*-methyl-D-aspartate receptor 2A signaling. Proc Natl Acad Sci USA 100:2854–2859.
Fleischmann A, Hvalby Ø, Jensen V, Strekalova T, Tacher C, Layer L, m Kvello A, Spanagel R, Sprengel R, Wagner EF, Gass P (2003) Impaired long-term memory and NR2A-type NMDA receptor dependent synaptic plasticity in mice lacking c-Fos in the brain. J Neurosci 23:9116–9122.
Flint AC, Maisch US, Weishaupt JH, Kriegstein AR, Monyer H (1997) NR2A subunit expression shortens NMDA receptor synaptic currents in developing neocortex. J Neurosci 17:2469–2476.
Fukaya M, Watanabe M (2000) Improved immunohistochemical detection of postsynaptically located PSD- 95/SAP90 protein family by protease section pretreatment: a study in the adult mouse brain. J Comp Neurol 426:572–586.
Gurd JW, Mahler HR (1974) Fractionation of synaptic plasma membrane glycoproteins by lectin affinity chromatography. Biochemistry 13:5193–5198.
Hardingham GE, Fukunaga Y, Bading H (2002) Extrasynaptic NMDARs oppose synaptic NMDARs by triggering CREB shut-off and cell death pathways. Nat Neurosci 5:405–414.
He Y, Janssen WG, Morrison JH (1998) Synaptic coexistence of AMPA and NMDA receptors in the rat hippocampus: a postembedding immunogold study. J Neurosci Res 54:444–449.
Husi H, Ward MA, Choudhary JS, Blackstock WP, Grant SG (2000) Proteomic analysis of NMDA receptor-adhesion protein signaling complexes. Nat Neurosci 3:661–669.
Ito I, Sakimura K, Mishina M, Sugiyama H (1996) Age-dependent reduction of hippocampal LTP in mice lacking *N*-methyl-D-aspartate receptor epsilon 1 subunit. Neurosci Lett 203:69–71.
Kennedy MB (2000) Signal-processing machines at the postsynaptic density. Science 290:750–754.
Khan AM, Curras MC, Dao J, Jamal FA, Turkowski CA, Goel RK, Gillard ER, Wolfsohn SD, Stanley BG (1999) Lateral hypothalamic NMDA receptor subunits NR2A and/or NR2B mediate eating: immunochemical/behavioral evidence. Am J Physiol 276:R880–R891.
Kirson ED, Yaari Y (1996) Synaptic NMDA receptors in developing mouse hippocampal neurones: functional properties and sensitivity to ifenprodil. J Physiol (Lond) 497:437–455.
Kiyama Y, Manabe T, Sakimura K, Kawakami F, Mori H, Mishina M (1998) Increased thresholds for long-term potentiation and contextual learning in mice lacking the NMDA-type glutamate receptor epsilon1 subunit. J Neurosci 18:6704–6712.
Klein RC, Prorok M, Galdzicki Z, Castellino FJ (2001) The amino acid residue at sequence position 5 in the conantokin peptides partially governs subunit-selective antagonism of recombinant *N*-methyl-D-aspartate receptors. J Biol Chem 276:26860–26867.
Koester HJ, Sakmann B (1998) Calcium dynamics in single spines during coincident pre- and postsynaptic activity depend on relative timing of back-propagating action potentials and subthreshold excitatory postsynaptic potentials. Proc Natl Acad Sci USA 95:9596–9601.
Kornau HC, Schenker LT, Kennedy MB, Seeburg PH (1995) Domain interaction between NMDA receptor subunits and the postsynaptic density protein PSD-95. Science 269:1737–1740.
Laemmli UK (1970) Cleavage of structural proteins during the assembly of the head of bacteriophage T4. Nature 227:680–685.
Laurie DJ, Bartke I, Schoepfer R, Naujoks K, Seeburg PH (1997) Regional, developmental and interspecies expression of the four NMDAR2 subunits, examined using monoclonal antibodies. Brain Res Mol Brain Res 51:23–32.
Li B, Chen N, Luo T, Otsu Y, Murphy TH, Raymond LA (2002) Differential regulation of synaptic and extra-synaptic NMDA receptors. Nat Neurosci 5:833–834.
Li BS, Sun MK, Zhang L, Takahashi S, Ma W, Vinade L, Kulkarni AB, Brady RO, Pant HC (2001) Regulation of NMDA receptors by cyclin-dependent kinase-5. Proc Natl Acad Sci USA 98:12742–12747.
Lu HC, Gonzalez E, Crair MC (2001) Barrel cortex critical period plasticity is independent of changes in NMDA receptor subunit composition. Neuron 32:619–634.
Lu W, Man H, Ju W, Trimble WS, MacDonald JF, Wang YT (2001) Activation of synaptic NMDA receptors induces membrane insertion of new AMPA receptors and LTP in cultured hippocampal neurons. Neuron 29:243–254.
Luo J, Wang Y, Yasuda RP, Dunah AW, Wolfe BB (1997) The majority of *N*-methyl-D-aspartate receptor complexes in adult rat cerebral cortex contain at least three different subunits (NR1/NR2A/NR2B). Mol Pharmacol 51:79–86.
Malenka RC, Nicoll RA (1999) Long-term potentiation—a decade of progress? Science 285:1870–1874.
Matsubara A, Laake JH, Davanger S, Usami S, Ottersen OP (1996) Organization of AMPA receptor subunits at a glutamate synapse: a quantitative immunogold analysis of hair cell synapses in the rat organ of Corti. J Neurosci 16:4457–4467.
McHugh TJ, Blum KI, Tsien JZ, Tonegawa S, Wilson MA (1996) Impaired hippocampal representation of space in CA1-specific NMDAR1 knockout mice. Cell 87:1339–1349.
Migaud M, Charlesworth P, Dempster M, Webster LC, Watabe AM, Makhinson M, He Y, Ramsay MF, Morris RG, Morrison JH, O'Dell TJ, Grant SG (1998) Enhanced long-term potentiation and impaired learning in mice with mutant postsynaptic density-95 protein. Nature 396:433–439.
Monyer H, Burnashev N, Laurie DJ, Sakmann B, Seeburg PH (1994) Developmental and regional expression in the rat brain and functional properties of four NMDA receptors. Neuron 12:529–540.
Nagelhus EA, Veruki ML, Torp R, Haug FM, Laake JH, Nielsen S, Agre P, Ottersen OP (1998) Aquaporin-4 water channel protein in the rat retina and optic nerve: polarized expression in Muller cells and fibrous astrocytes. J Neurosci 18:2506–2519.
Nusser Z (2000) AMPA and NMDA receptors: similarities and differences in their synaptic distribution. Curr Opin Neurobiol 10:337–341.
Petralia RS, Esteban JA, Wang YX, Partridge JG, Zhao HM, Wenthold RJ, Malinow R (1999) Selective acquisition of AMPA receptors over postnatal development suggests a molecular basis for silent synapses. Nat Neurosci 2:31–36.
Philpot BD, Sekhar AK, Shouval HZ, Bear MF (2001) Visual experience and deprivation bidirectionally modify the composition and function of NMDA receptors in visual cortex. Neuron 29:157–169.
Racca C, Stephenson FA, Streit P, Roberts JD, Somogyi P (2000) NMDA receptor content of synapses in stratum radiatum of the hippocampal CA1 area. J Neurosci 20:2512–2522.
Rossi P, Sola E, Taglietti V, Borchardt T, Steigerwald F, Utvik JK, Ottersen OP, Köhr G, D'Angelo E (2002) NMDA receptor 2 (NR2) C-terminal control of NR open probability regulates synaptic transmission and plasticity at a cerebellar synapse. J Neurosci 22:9687–9697.
Sabatini BL, Oertner TG, Svoboda K (2002) The life cycle of Ca^{2+} ions in dendritic spines. Neuron 33:439–452.
Sakimura K, Kutsuwada T, Ito I, Manabe T, Takayama C, Kushiya E, Yagi T, Aizawa S, Inoue Y, Sugiyama H, et al (1995) Reduced hippocampal LTP and spatial learning in mice lacking NMDA receptor epsilon 1 subunit. Nature 373:151–155.
Sans N, Petralia RS, Wang YX, Blahos II J, Hell JW, Wenthold RJ (2000) A

developmental change in NMDA receptor-associated proteins at hippocampal synapses. J Neurosci 20:1260–1271.
Sans N, Prybylowski K, Petralia RS, Chang K, Wang YX, Racca C, Vicini S, Wenthold RJ (2003) NMDA receptor trafficking through an interaction between PDZ proteins and the exocyst complex. Nat Cell Biol 5:520–530.
Sattler R, Xiong Z, Lu WY, MacDonald JF, Tymianski M (2000) Distinct roles of synaptic and extrasynaptic NMDA receptors in excitotoxicity. J Neurosci 20:22–33.
Sheng M, Kim MJ (2002) Postsynaptic signaling and plasticity mechanisms. Science 298:776–780.
Sheng M, Pak DT (2000) Ligand-gated ion channel interactions with cytoskeletal and signaling proteins. Annu Rev Physiol 62:755–778.
Sheng M, Cummings J, Roldan LA, Jan YN, Jan LY (1994) Changing subunit composition of heteromeric NMDA receptors during development of rat cortex. Nature 368:144–147.
Sprengel R, Suchanek B, Amico C, Brusa R, Burnashev N, Rozov A, Hvalby O, Jensen V, Paulsen O, Andersen P, Kim JJ, Thompson RF, Sun W, Webster LC, Grant SG, Eilers J, Konnerth A, Li J, McNamara JO, Seeburg PH (1998) Importance of the intracellular domain of NR2 subunits for NMDA receptor function in vivo. Cell 92:279–289.
Steigerwald F, Schulz TW, Schenker LT, Kennedy MB, Seeburg PH, Köhr G (2000) C-Terminal truncation of NR2A subunits impairs synaptic but not extrasynaptic localization of NMDA receptors. J Neurosci 20:4573–4581.
Stocca G, Vicini S (1998) Increased contribution of NR2A subunit to synaptic NMDA receptors in developing rat cortical neurons. J Physiol (Lond) 507:13–24.
Takumi Y, Ramirez-Leon V, Laake P, Rinvik E, Ottersen OP (1999) Different modes of expression of AMPA and NMDA receptors in hippocampal synapses. Nat Neurosci 2:618–624.
Tang YP, Shimizu E, Dube GR, Rampon C, Kerchner GA, Zhuo M, Liu G, Tsien JZ (1999) Genetic enhancement of learning and memory in mice. Nature 401:63–69.
Tezuka T, Umemori H, Akiyama T, Nakanishi S, Yamamoto T (1999) PSD-95 promotes Fyn-mediated tyrosine phosphorylation of the N-methyl-D-aspartate receptor subunit NR2A. Proc Natl Acad Sci USA 96:435–440.
Tovar KR, Westbrook GL (1999) The incorporation of NMDA receptors with a distinct subunit composition at nascent hippocampal synapses *in vitro*. J Neurosci 19:4180–4188.
Valtschanoff JG, Weinberg RJ (2001) Laminar organization of the NMDA receptor complex within the postsynaptic density. J Neurosci 21:1211–1217.
Walikonis RS, Jensen ON, Mann M, Provance DW Jr, Mercer JA, Kennedy MB (2000) Identification of proteins in the postsynaptic density fraction by mass spectrometry. J Neurosci 20:4069–4080.
Wigstrom H, Gustafsson B (1985) Facilitation of hippocampal long-lasting potentiation by GABA antagonists. Acta Physiol Scand 125:159–172.
Wong RW, Setou M, Teng J, Takei Y, Hirokawa N (2002) Overexpression of motor protein KIF17 enhances spatial and working memory in transgenic mice. Proc Natl Acad Sci USA 99:14500–14505.
Yaka R, Thornton C, Vagts AJ, Phamluong K, Bonci A, Ron D (2002) NMDA receptor function is regulated by the inhibitory scaffolding protein, RACK1. Proc Natl Acad Sci USA 99:5710–5715.
Yasuda H, Barth AL, Stellwagen D, Malenka RC (2003) A developmental switch in the signaling cascades for LTP induction. Nat Neurosci 6:15–16.
Yoshimura Y, Ohmura T, Komatsu Y (2003) Two forms of synaptic plasticity with distinct dependence on age, experience, and NMDA receptor subtype in rat visual cortex. J Neurosci 23:6557–6566.
Yuste R, Majewska A, Cash SS, Denk W (1999) Mechanisms of calcium influx into hippocampal spines: heterogeneity among spines, coincidence detection by NMDA receptors, and optical quantal analysis. J Neurosci 19:1976–1987.
Zamanillo D, Sprengel R, Hvalby O, Jensen V, Burnashev N, Rozov A, Kaiser KM, Koster HJ, Borchardt T, Worley P, Lubke J, Frotscher M, Kelly PH, Sommer B, Andersen P, Seeburg PH, Sakmann B (1999) Importance of AMPA receptors for hippocampal synaptic plasticity but not for spatial learning. Science 284:1805–1811.